Japan Bilingual Publishing Co.

New Environmentally-Friendly Materials

https://ojs.bilpub.com/index.php/nefm

ARTICLE

Synthesis and Antimicrobial Properties Pectin + CuNi Films and Characterization by Scanning Electron Microscopy

Yamila Illanez [1] ***, Corina Cangiano*** [1] ***, Yesica Sabrina Lambrese*** [1,2] ***, Cecilia Fernandez*** [1] ***, Marcelo Ricardo Esquivel*** [3,4*] ***, Maria de los Ángeles Cangiano*** [1,5]

[1] *Facultad de Ingeniería y Ciencias Agropecuarias, Universidad Nacional de San Luis, Villa Mercedes 5730, Argentina*

[2] *Instituto Nacional de Tecnología Industrial (INTI) San Luis, San Luis 5700, Argentina*

[3] *Departamento de Química, Universidad Nacional del Comahue, Bariloche 8400, Argentina*

[4] *Departamento de Caracterización de Materiales, Comisión Nacional de Energía Atómica (CNEA) y Consejo Nacional de Investigaciones Científicas y Técnicas (CONICET), Bariloche 8400, Argentina*

[5] *Instituto de Tecnología Química Universidad Nacional de San Luis (UNSL) y Consejo Nacional de Investigaciones Cientificas y Técnicas (CONICET) , Villa Mercedes 5370, Argentina*

ABSTRACT

The synthesis of pectin-based films containing nanoparticles of CuNi (NPs), with potential antimicrobial properties, as an active solid is presented in this work. The NPs were dispersed in pure pectin to be used as food packaging in the food industry. The samples obtained were laid flat to characterize the sample thickness. The goal of this work is to find appropriate electron microscopy techniques to characterize the dispersion of the NPs on the pectin film and the pectin microstructural and antimicrobial characteristics properly. Different microstructural techniques of scanning electron microscopy modes were used to study the films, including low-voltage scanning electron microscopy (SEM) and low-voltage energy-dispersive spectroscopy (EDS). The condition of low beam voltage allows the sample characterization without destroying the sample surface/bulk due to electron irradiation. The pectin films containing raw NPs (pectin +

*CORRESPONDING AUTHOR:

Marcelo Ricardo Esquivel, Departamento de Química, Universidad Nacional del Comahue, Bariloche 8400, Argentina; Departamento de Caracterización de Materiales, Comisión Nacional de Energía Atómica (CNEA) y Consejo Nacional de Investigaciones Científicas y Técnicas (CONICET), Bariloche 8400, Argentina; Email: marceloesquivel@cnea.gob.ar or marcelo.esquivel@crub.uncoma.edu.ar

ARTICLE INFO

Received: 12 September 2025 | Revised: 15 October 2025 | Accepted: 22 October 2025 | Published Online: 29 October 2025

DOI: https://doi.org/10.55121/nefm.v4i2.711

CITATION

Illanez, Y., Cangiano, C., Lambrese, Y.S., et al., 2025. Synthesis and Antimicrobial Properties Pectin + CuNi Films and Characterization by Scanning Electron Microscopy. New Environmentally-Friendly Materials. 4(2): 68–78. DOI: https://doi.org/10.55121/nefm.v4i2.711

NPs) and milled NPs (pectin + milled NPs) were observed by SEM in two different image modes: secondary electrons (SE) and backscattered electrons (BSE). The last mode allows the identification of sample components, i.e., matrix + samples containing different atomic Z numbers. This fact allows us to know the distribution of the metal particles within the volume of the sample. The results obtained in this work are relevant for the characterization and further use of these films in the protection of snacks in the food industry.

Keywords: Pectin; Scanning Electron Microscopy; Energy Dispersive Spectroscopy; Cuni Nanoparticles; Food Packaging

1. Introduction

Currently, the interest in pectin-based films is increasing for their potential application as environmentally friendly packaging in the food industry [1]. Pectin is naturally occurring and biodegradable, and due to its gelling and thickening features, it can absorb water and be tailored to obtain a thin film. These films are flexible enough to be tunable with the incorporation of bioactive agents such as nanocellulose, zinc oxide, silver, and multiple metal particles [2–4].

These films present two main components:

- The matrix is composed of pectin with poor mechanical strength and low water barrier properties [5]. As a film, pectin offers support for the nanoparticles and a protective covering for the food industry.
- Nanoparticles. The addition of these nanoparticles often increases the pectin film's mechanical strength, water barrier properties, and antimicrobial activity [6–8]. These nanoparticles reinforced the properties of the pectin films as protective coverings for the food industry.

In this work, commercial citric pectin and glycerol are selected to obtain a liquid. The CuNi particles were added to this liquid phase. This combined phase was laid as a thin film on a flat plaque and dried at temperatures higher than ambient.

This methodology was selected due to the possibility of extending this laboratory layout scheme to a larger scale of additive manufacturing controlled by 3D printing nozzles containing the liquid phase over temperature-controlled printing beds [9].

Nevertheless, the main problem of the study of any composite, such as films containing particles, is complex. It is due to the simultaneous determination of the microstructure features of two components with very distinctive properties: a very dense conductive metal/alloy and a non-conductive light structure composed of polysaccharides with low resistance to localized electron irradiation.

Among others, scanning electron microscopy and associated techniques offer the possibility of the simultaneous characterization of these two components in order to determine the thickness, surface characteristics, particle size, elemental composition, and particles within the sample. This is possible by combining imaging in different modes and spectral analysis at different voltages. These operating conditions associated with the simulation of the structure are used to complete the sample study.

Then, the main objective of this paper is to obtain an appropriate microstructural characterization of the two components of the films by scanning electron microscopy and associated techniques and the antimicrobial activity. The potential use in the food packaging industry justifies the effort since SEM can be used as a regular technique to establish a quality marker of the characteristics of the manufactured pectin + NP films.

2. Materials and Methods

2.1. Preparation of the CuNi Nanoparticles

The CuNi particles of this study were synthesized by the sol-gel method from the corresponding nitrates in a 1:1 molar ratio. Citric acid solutions were added to different aliquots of a liquid solution containing the Cu^{2+} and Ni^{2+} ions in order to obtain a molar ratio of C/Me = 0.73. In this ratio, C is the amount of moles of citric acid and Me is the sum of the amount of moles of both Ni and Cu. Once the solution was obtained, it was heated at 60 °C and under vacuum to obtain a viscous gel. After that, the sample was

gradually heated in a laboratory oven from room temperature up to 100 °C to obtain the solid precursors. Then, the solids were heated and reduced to finally reach the CuNi nanoparticles. Details of this synthesis method are explained elsewhere [10]. This synthesis method was selected because it is popularly used to obtain nanoparticles of metals and alloys [11,12]. There are other successful methods currently used to obtain metal nanoparticles in pectin or other polymer-based matrices such as pectin-based and cotton fabrics [13–15]. Preparation methods include the synthesis of CuNP´s using S. cumini leaf extract [13]. The method takes advantage of the role of tannin, phenols, alkaloids and flavonoids as reducing and capping agents in synthesizing the CuNPs [13]. Other synthesis methods include the use of the functional groups like carboxylic acid and hydroxyl present in pectin [14]. These groups make the matrix of pectin suitable to be covalently bonded with other proteins or biomolecules [14]. Then, pectin is being extensively used to either coat or encapsulate metal/alloys nanoparticles (MNPs) in order to inhibit their aggregation properties [14]. In this way, the pectin increases the possible use of MNPs for antimicrobial activity and drug delivery [14]. Synthesis methods also involve the coprecipitation using citrus pectin and sol-gel methods to obtain Fe/Cu NPs [15]. The main result obtained is that Cu and Fe NP's offer both catalytic activity and effective electron transfer processes and the pectin coating improve the stability and adsorption capacity [15]. The NP's + pectin matrix is used in wastewater treatment applications [15].

2.2. Preparation of Bioactive Films

The pectin films were prepared from pure citric commercial pectin of 2% m/m with a 70% esterification percentage and a 140 Dka molecular weight and commercial (Ciccarelli, 99.5% purity) glycerol of 1% m/p dissolved in pure distilled water. The resulting solution was stirred at 250 rpm at room temperature. The resulting thin film was laid on flat glass petri dishes. This film was called reference pectin. Both milled and unmilled CuNi particles were added to the pectin + glycerol mixture.

The CuNi + pectin films were prepared the same way.

The films containing both milled and milled CuNi particles + pectin and reference pectin films are analyzed in this work.

2.3. Scanning Electron Microscopy Characterization

The thin films were studied by scanning electron microscopy using a FEI INSPECT S50 thermionic microscope operated between 100 V and 30 kV. The emissive mode is measured by selecting the signal obtained in a standard Everthart Thornley Detector (EDT). The signal is used to study the superficial features obtained from the analysis of the inelastic interaction of the electrons of the primary beam with the sample [16,17]. Low primary beam voltage and current were selected to avoid damage to the pectin sample surface. Selected values are lower than 5 kV. Reflective mode is measured by selecting the signal obtained in the vCD detector located around the microscope pole piece. This mode analyzes the elastic interaction of the primary beam with the sample. As a result of this interaction, compounds with different average atomic number (Z) can be identified, leading to an imaging mode with compositional contrast [18–20]. If needed, higher voltages were used.

The energy dispersive spectroscopy (EDS) measurements were done with an EDAX Octane Pro detector using a 10 mm^2 window area. Measurements were done with a minimum of 1000 cps (counts per second) with dead times lower than 20% and voltages between 5 and 20 kV. Operating conditions were selected in order to identify the elements and simultaneously trying to avoid sample damage due to electron beam irradiation [21,22].

Electron trajectories within the solid sample were simulated by using CASINO ™ software in order to analyze the imaging and EDS results [23–25].

2.4. Microbiological Analysis and Antimicrobial Activity Assays

Microbial contamination in control pectin films, without the addition of nanoparticles, was evaluated using Petri dishes of 24.5 mm diameter and 15.5 mm depth. containing a culture medium supplemented with 10% glucose and 5% yeast extract. The films were placed directly onto the inoculated media and incubated at 25 °C for 24 h. All assays were performed in triplicate. The presence of visible microbial growth on the plates was considered indicative of microbial contamination.

In addition, the antifungal activity of pectin-based films incorporating unmilled and milled CuNi nanoparticles was evaluated against phytopathogenic fungi. Strains of *Alternaria* sp., *Fusarium* sp., and *Penicillium expansum* INTA 5 were cultured in the same medium (10% glucose and 5% yeast extract) at 25 °C for 4 days. Conidia were harvested and suspended in 10 mL of sterile distilled water containing 0.055% (v/v) Tween 80 in order to prevent aggregation. The concentration of conidia in the suspension was determined using a Neubauer chamber and adjusted to 5×10^6 conidia mL^{-1}.

Aliquots of 100 µL of each conidial suspension were evenly spread onto solid culture media in Petri dishes. After a 10 min absorption period, the films were placed on the agar surface, and the plates were incubated at 25 °C for 7 days. All experiments were carried out in triplicate. Antifungal activity was expressed as mycelial growth inhibition (MGI), evaluated after 7 days of incubation. The presence of inhibition zones around the films was considered indicative of fungal growth inhibition; in cases where the inhibition halo exceeded 10 mm around the film, complete inhibition (100%) was assumed, whereas total fungal overgrowth on the film surface was considered as 0% inhibition.

3. Results and Discussion

3.1. Scanning Electron Microscopy Characterization

3.1.1. Emissive Mode

Figure 1 shows a mosaic of SEM images obtained by using an ETD standard detector under different beam voltages (2 and 10 kV). **Figure 1a** shows the surface of the pectin reference sample. The image is obtained by using 2 kV. It is less damaged than the one obtained using 10 kV. Therefore, voltages of 2 kV or less at times shorter than 30 s were used to characterize the pectin film. These differences in imaging quality are due to beam electron irradiation which is proportional to both time of exposure and beam current. The beam current in the thermionic microscope used in this work is proportional to both voltage and spot.

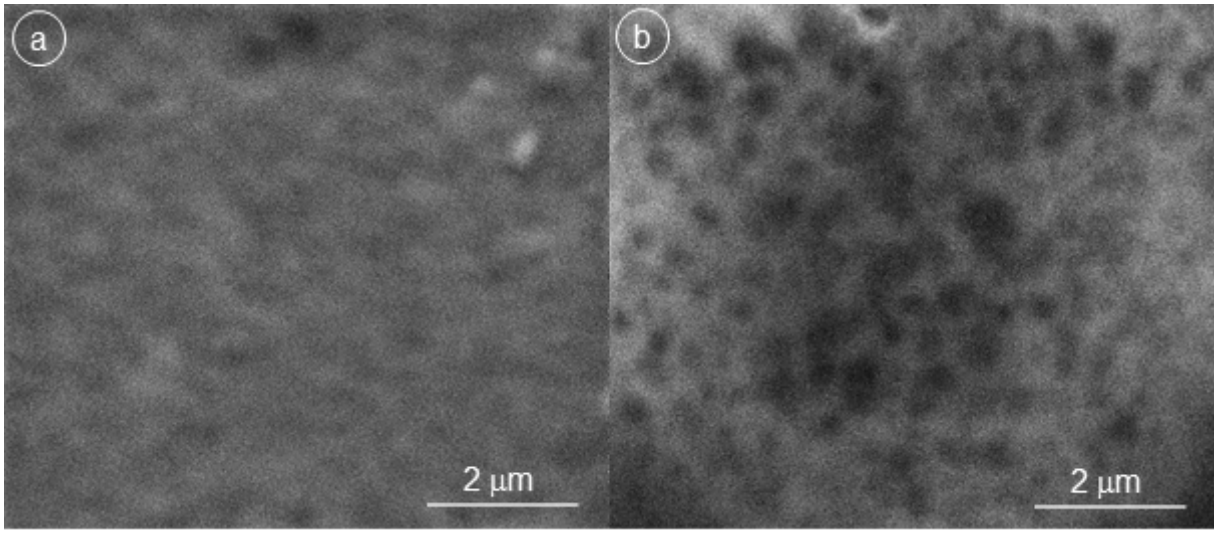

Figure 1. SEM images from secondary electrons of reference pectin film: (**a**) 2 kV for 5 min; (**b**) 10 kV for 5 min.

Then, the SEM characterization is made by focusing on a different zone where the image is obtained. Samples were not sputtered with Au or equivalent treatment, and the use of low electron beam voltage allows the imaging and fulfills Thevenin's condition without charging the sample [26,27].

Figure 2 shows a mosaic of SEM images on the reference pectin film at 2 kV. This voltage value minimizes the damage to the film surface. As observed, no highly marked superficial contrast is detected in **Figure 2a**. It indicates a completely flat surface. In this image, the surface is perpendicular to the angle of incidence of the beam. At

higher voltages and longer exposure times, the primary beam affects the sample, and the effects of irradiation due to the scattering of the electrons on the sample bulk produce damage on the pectin surface, as shown in **Figure 1**. This effect is reported in polymer-based materials [28 30]. As a result, pits and holes are produced. Then, the actual starting material loses its former characteristics. The same sample is shown in **Figure 2b**. In this figure, the sample is tilted at 50° (degrees) with respect to the position shown in **Figure 2a**. A tilted position is selected in order to verify the sample roughness. It is possible because the production of secondary electrons (ε) depends on the angle between the sample and the incident electron beam according to Equation (1) [31]. In this equation, ε(θ) is the production of secondary electrons as a function of the angle between the perpendicular to the direction of the incident beam and the tilting angle of the sample. ε(0) is the production of secondary electron when the electron beam is perpendicular to the sample, and sec(θ) is the secant function of the (è values.

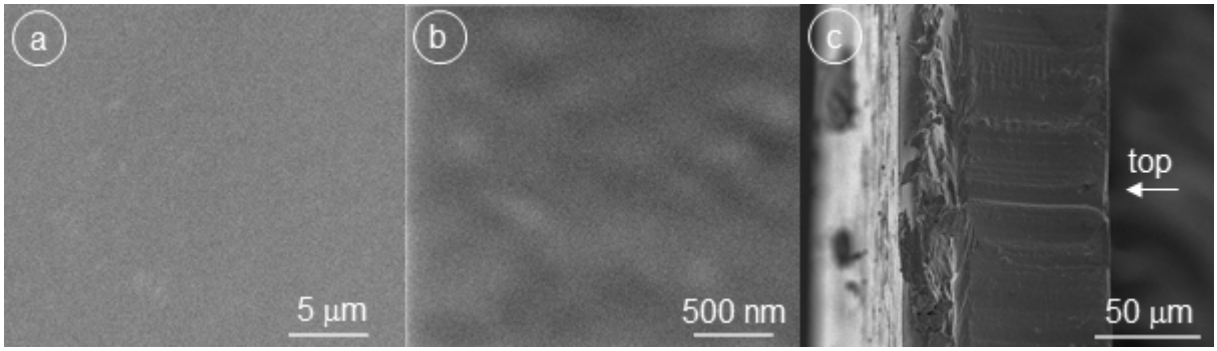

Figure 2. SEM images from secondary electrons of control pectin: (**a**) Surface normal to the electron beam; (**b**) Tilted surface at 50° with respect to **Figure 2a**; (**c**) The side of the pectin sample.

$$\varepsilon(\theta) = \varepsilon(0) \times \sec(\theta). \quad (1)$$

Then, tilting the sample is a better approach to determine the presence of surface defects. As observed in **Figure 2b**, the sample is quite smooth with no contrast event at tilting values of 50 degrees. **Figure 2c** shows an SEM image where the thickness of the reference pectin film is observed. An average value of ~100 m is shown with a scale. The surface of **Figure 2c** corresponds to the side of the sample, which is not smooth, indicating that the drying procedure leads to the formation of rough layers on the border of the sample. The top label of **Figure 2c** corresponds to the upper surface shown in images **Figure 2a,b**.

Figure 3 shows the simulation of the electron beam interaction with the solid pectin film at 2 kV and 20 kV using CASINO ™ [23].

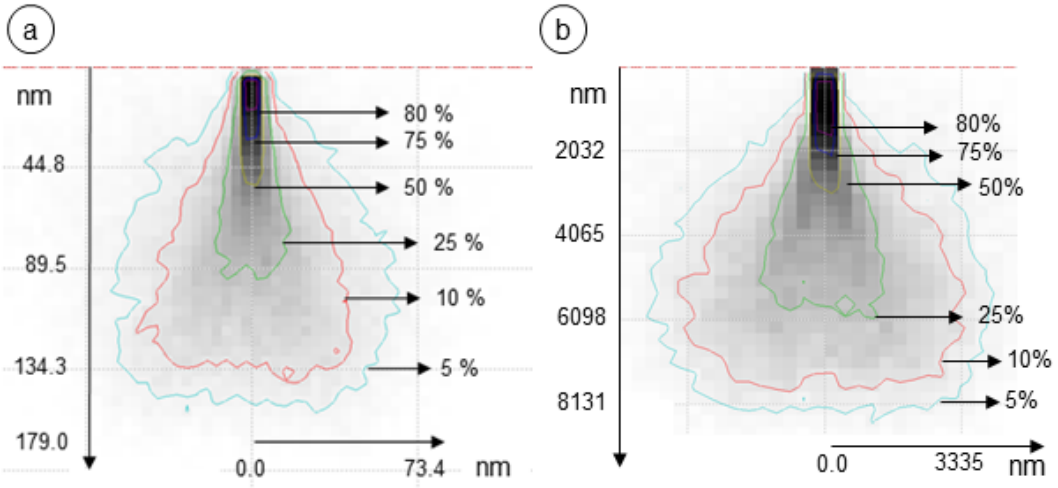

Figure 3. Simulation of the primary electron beam interaction with the solid pectin film: (**a**) 2 kV; (**b**) 20 kV.

The figure displays the Energy lost by the electrons of the primary ion beam as the electron–sample interaction takes place. Energy lost is proportional to the depth of the sample. The different percentages indicate the remaining amount from the starting initial beam voltage value. As observed in **Figure 3a**, the initial 2 kV beam loses almost 95% of its energy at a depth of ~160 nm. Unlike this value, the initial 20 kV beam loses its energy at a depth of ~8131 nm as observed in **Figure 3b**. This means that images obtained at higher voltage values show an average of the signal of the different layers of the films. Therefore, a beam voltage of 2kV and lower current is the best condition to capture the film surface images with minimum damage and at shorter depths.

Figure 4 shows a mosaic of SEM images of the pectine + milled CuNi films. **Figure 4a** shows the surface of the sample. The electron beam voltage used is 2 kV. No damage to the surface is observed. **Figure 4b** shows the side of the film. An average value of the film of ~70 m is observed. Notice the roughness of the film side evidenced the fact that both images were obtained at the same conditions.

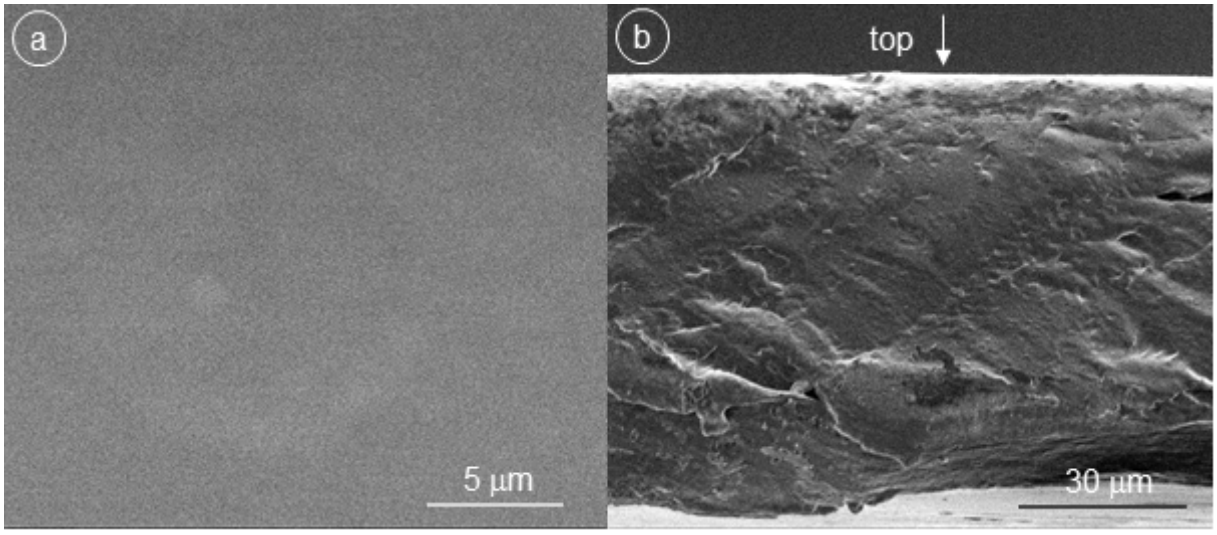

Figure 4. SEM images from secondary electrons of the control pectin sample: (**a**) Sample perpendicular surface to the electron beam; (**b**) Sample side surface.

3.1.2. Reflective Mode

Figure 5 shows a mosaic of SEM images of the pectine + milled CuNi films using a vCD-detector. The detector is set around the pole piece. In this way, the detector surrounds the primary electron beam. The detector is located in this position to take advantage of the different production of backscattered electrons from the atoms present in the sample. This value is usually called η. The η production depends only on the Z number of the elements that constitute the sample, provided that voltage and current of the beam are maintained as a constant value.

In this mode, Cu and Ni atoms have a higher backscattered electron production than C, N, and O, the main atoms present in the pectin compound. This difference is observed as a bright difference in the image. The brighter zone corresponds to zones where elements with higher Z are located.

As observed in **Figure 5b**, there are differences in image contrast. The bright differences correspond to zones where Cu-Ni nanoparticles are located. Two voltages were used to determine the presence of CuNi nanoparticles. No clear contrast between Cu-Ni nanoparticles and pectin film is observed at 5 kV, as shown in **Figure 5a**. The contrast is clear and obvious at 10 kV as observed in **Figure 5b**. Nevertheless, the surface is damaged at 10 kV as shown in the SEM image. The damage on the surface leads to the formation of pits and holes on the surface and bulk of the sample. It is clearly observed by the backscattered electron signal because the signal also depends on the electron travelling across the sample, induced by the beam material interaction [28–34]. This means that the gray degree in con-

trast along the sample evidences differences in Z contrast, density, and topography [32–34]. These differences in density were introduced by the electron beam damage and appreciated by the electron backscattered signal [28–30]. As observed in **Figure 4b**, the size of the Cu-Ni nanoparticles is below 200 µm. This value is similar to those obtained in similar synthesis methods [13,14]. The similarities are related to the fact that NP sizes are not defined by the matrix-type but by the synthesis method itself.

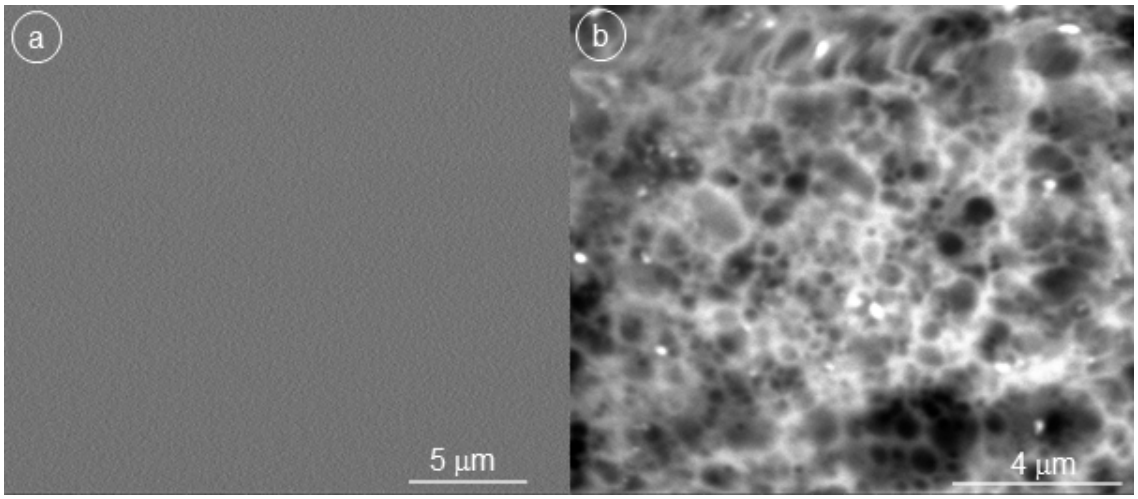

Figure 5. SEM mosaic images of pectin + CuNi nanoparticles using backscattered electrons: (**a**) 5 kV; (**b**) 10 kV.

3.2. Energy Dispersive Spectroscopy Characterization

Figure 6 shows energy-dispersive measurements done on the bright rounded spots of **Figure 5b**. The measurements were done at 5 kV to avoid the sample damage. The presence of the CuNi nanoparticles was identified in the sample. The L characteristic family lines of Cu and Ni are observed in **Figure 6**. At these voltages, each L line is not resolved. The K characteristic lines of C, N and O are also observed. These elements are the main components of pectin.

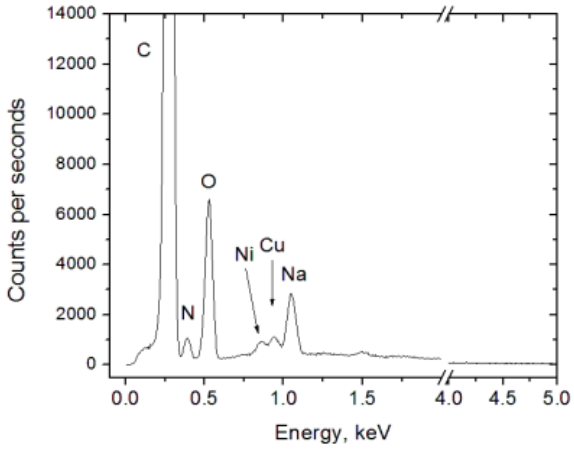

Figure 6. EDS measurement on the bright points of **Figure 4b**.

The EDS measurement of **Figure 6** is also an interesting result. Instead of using the characteristic K lines of Cu and Ni, we use the L characteristic lines of both elements. This fact not only allows us to identify Ni and Cu at a beam voltage of 5 kV but also avoids the sample surface and bulk damage. The EDS signal also identifies C, O, and N K characteristic lines at this voltage value.

3.3. Antimicrobial Properties

Figure 7 shows the presence of microbial contamination on the control pectin film (without nanoparticle addition) after 3 days of cultivation on plates containing different fungal pathogens, as well as the antimicrobial activity of two polymeric matrices based on the incorporation of unmilled and milled CuNi nanoparticles after 7 days of incubation with the evaluated microorganisms. The control pectin film (sample 1, identified as number 1) did not show microbial growth either on the film surface or in the surrounding agar in plates inoculated with *Alternaria* sp. or *Fusarium* sp. during the first 3 days of incubation, indicating the absence of fungal development. These observations confirm the lack of microbial contamination in the biopolymeric matrices evaluated. Regarding the antimicrobial properties of the films, those containing unmilled CuNi

nanoparticles (film samples identified as number 6 in **Figure 7d–f**) exhibited inhibition zones on plates inoculated with *Fusarium* sp. after 7 days of incubation, indicating a significant antifungal effect. Similar antimicrobial behavior has been previously reported for copper-based pectin films used in smart packaging applications [35–37]. On the other hand, pectin films containing milled CuNi nanoparticles (film samples identified as number 7 in **Figure 7d–f**) showed localized variations in fungal growth density. Specifically, inhibition zones with halos larger than 10 mm, corresponding to complete inhibition (100%), were observed on plates inoculated with *Alternaria* sp., whereas a poorly defined inhibitory effect, without the formation of halos suitable for quantitative measurement, was observed on plates inoculated with *Fusarium* sp. after 7 days of cultivation. In all cases, no antifungal activity was observed against *Penicillium expansum* INTA-5 under the experimental conditions evaluated. These results suggest that the antimicrobial performance of the films is strongly influenced by the physical state of the CuNi nanoparticles and is also dependent on the type of microorganism evaluated. The milling process may induce surface oxidation or structural modifications in the CuNi nanoparticles, potentially limiting the release or bioavailability of active metallic species. The effect of particle milling on antimicrobial activity is currently under investigation [37,38].

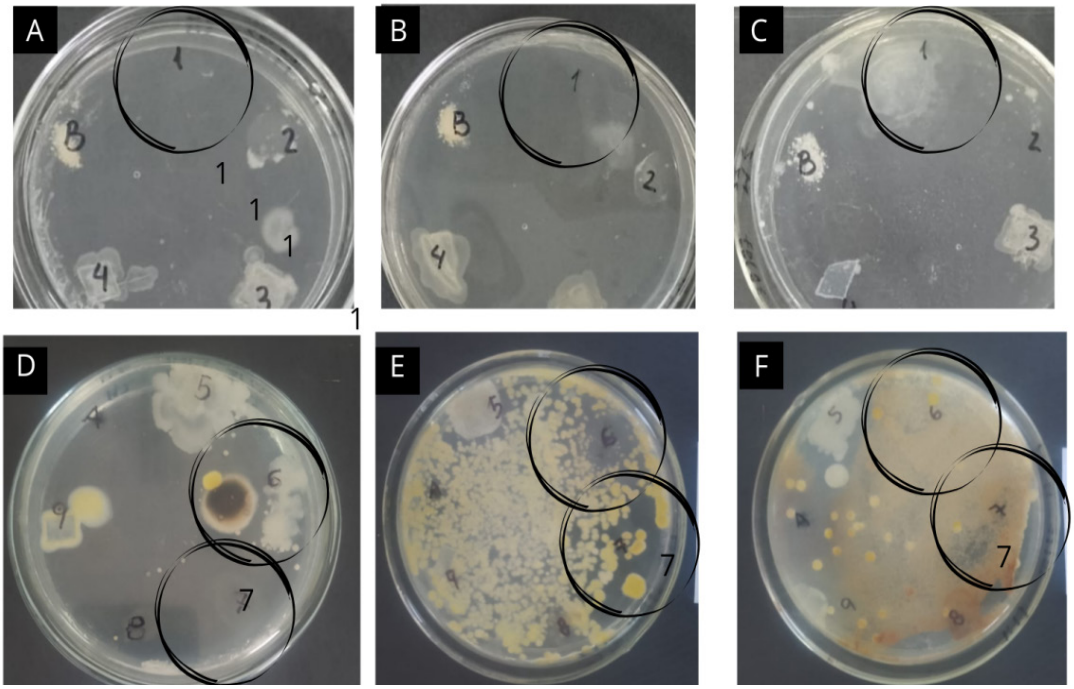

Figure 7. Microbial contamination observed on the control pectin film (without nanoparticle addition) after 3 days of cultivation, and antimicrobial activity of pectin-based films incorporating unmilled and milled CuNi nanoparticles against fungal pathogens after 7 days of incubation: (**a, d**) agar plates inoculated with *Alternaria* sp.; (**b, e**) agar plates inoculated with *Fusarium* sp.; (**c, f**): agar plates inoculated with *Penicillium expansum* INTA-5.

Note: Circles indicate the position of the films on the agar surface: control pectin film (sample 1), pectin film containing unmilled CuNi nanoparticles (sample 6), and pectin film containing milled CuNi nanoparticles (sample 7).

4. Conclusions

The fabrication of flat and smooth films of pectin containing CuNi nanoparticles from a liquid phase, followed by drying at ambient conditions on a petri dish, is a worthwhile synthesis method. This experimental methodology can be scaled up by using a similar set-up based on 3D printing. The characterization of the product is successfully done by SEM imaging using emissive and reflective modes. The use of low-voltage electron beam values allows observing the actual surface of the pectin films without destroying their properties. At higher voltages, the electron beams impinging energy and current only damage both the surface and bulk of the film [24–26,28]. This

assessment is verified both experimentally and by simulation of the electron beam-film interaction. The presence of the CuNi nanoparticles in the pectin films is verified by electron backscattered imaging and EDS measurements. The antifungal properties were measured by analyzing the inhibition halo for all the strains of fungi observed. It is observed that the films of pectin + non-milled CuNi nanoparticles present interesting antimicrobial properties, demonstrating the feasibility of use in food industry packaging.

Author Contributions

Conceptualization, methodology, validation, formal analysis, investigation, Y.I., C.C., Y.S.L., C.F., M.R.E. and M.d.l.A.C.; writing—original draft preparation, writing—review and editing, visualization, supervision, project administration, funding acquisition, C.F., M.R.E. and M.d.l.A.C. All authors have read and agreed to the published version of the manuscript.

Funding

This study was partially funded by Universidad Nacional del Comahue (Project 04/B246), Universidad Nacional de San Luis and CONICET.

Institutional Review Board Statement

Not applicable.

Informed Consent Statement

Not applicable.

Data Availability Statement

The authors are willing to share research data via the e-mail specified above.

Conflicts of Interest

The authors declare no conflict of interest.

References

[1] Freitas, C.M.P., Coimbra, J.S.R., Souza, V.G.L., et al., 2021. Structure and Applications of Pectin in Food, Biomedical and Pharmaceutical Industry: A Review. Coatings. 11(8), 922–944. DOI: https://doi.org/10.3390/coatings11080922

[2] Chaichi, M., Hashemi, M., Badii, F., et al., 2017. Preparation and Characterization of a Novel Bionanocomposite Edible Film Based on Pectin and Crystalline Nanocellulose. Carbohydrate Polymers. 157, 167–175. DOI: https://doi.org/10.1016/j.carbpol.2016.09.062

[3] Hari, K.D., Garcia, C.V., Shin, G.-H., et al., 2021. Improvement of the UV Barrier and Antibacterial Properties of Crosslinked Pectin/Zinc Oxide Bionanocomposite Films. Polymers. 13(15), 2403. DOI: https://doi.org/10.3390/polym13152403

[4] Hileuskaya, K., Ladustka, A., Kulikouskaya, V., et al., 2020. 'Green' Approach for obtaining Stable Pectin-Capped Silver Nanoparticles: Physico-Chemical Characterization and Antibacterial Activity. Colloids and Surfaces A: Physicochemical and Engineering Aspects. 585, 124141. DOI: https://doi.org/10.1016/j.colsurfa.2019.124141

[5] Souza, V.G.L., Mello, I.P., Khalid, O., et al., 2022. Strategies to Improve the Barrier and Mechanical Properties of Pectin Films for Food Packaging: Comparing Nanocomposites with Bilayers. Coatings. 12(2), 108.

[6] Suyatma, N.E., Ishikawa, Y., Kitazawa, H., 2013. Nanoreinforcement of Pectin Film to Enhance Its Functional Packaging Properties by Incorporating ZnO Nanoparticles. Advanced Materials Research. 845, 451–456. DOI: https://doi.org/10.4028/www.scientific.net/AMR.845.451

[7] El Habbasha, E.S., Abouzeid, R., Ibrahim, F.M., et al., 2025. Developing a Novel, Low-Cost, Antimicrobial, and Biodegradable Pectin/HEC/ZnO Biofilm for Edible Food Packaging Applications. Biomass Conversion and Biorefinery. 15, 6377–6388. DOI: https://doi.org/10.1007/s13399-024-05487-4

[8] Zhang, S., Cheng, X., Fu, Q., et al., 2023. Pectin–Nanolignin Composite Films with Water Resistance, UV Resistance, and Antibacterial Activity. Food Hydrocolloids. 143, 108783. DOI: https://doi.org/10.1016/j.foodhyd.2023.108783

[9] Agarwal, T., Costantini, M., Maiti, T.K., 2021. Extrusion 3D Printing with Pectin-Based Ink Formulations: Recent Trends in Tissue Engineering and Food Manufacturing. Biomedical Engineering

Advances. 2, 100018. DOI: https://doi.org/10.1016/j.bea.2021.100018

[10] Cangiano, M.d.l.A., Ojeda, M.W., Carreras, A.C., et al., 2010. A Study of the Composition and Microstructure of Nanodispersed Cu–Ni Alloys Obtained by Different Routes from Copper and Nickel Oxides. Materials Characterization. 61(11), 1135–1146. DOI: https://doi.org/10.1016/j.matchar.2010.07.006

[11] Romanova, I., Kirillov, S., 2018. Preparation of Cu, Ni and Co Oxides by a Citric Acid-Aided Route. Journal of Thermal Analysis and Calorimetry. 132, 503–512. DOI: https://doi.org/10.1007/s10973-017-6880-5

[12] Cangiano, M.d.l.A., Ojeda, M.W., Ruiz, M.d.C., 2015. Effect of pH Value and Calcination Temperature on Synthesis and Characteristics of Cu–Ni Nano-Alloys. Transactions of Nonferrous Metals Society of China. 25(11), 3664–3677. DOI: https://doi.org/10.1016/S1003-6326(15)64008-0

[13] Boruah, G., Phukan, A.R., Kalita, B., et al., 2025. Antimicrobial and UV Protection Finishing of Cotton Fabric with Copper Nanoparticles Synthesized Using S. cumini Leaf Extract. Clean Technologies and Environmental Policy. 27, 2043–3053. DOI: https://doi.org/10.1007/s10098-024-02933-9

[14] Nemiwal, M., Zhang, T.C., Kumar, D., 2021. Pectin Modified Metal Particles and Their Application in Property Modification of Biosensors. Carbohydrate Polymer Technologies and Applications. 2, 100164. DOI: https://doi.org/10.1016/j.carpta.2021.100164

[15] Hassan, F., Talib, U., Saif, S., et al., 2024. Pectin Functionalized with Cu/Fe Nanoparticles for Enhanced Degradation of Methylene Blue from Wastewater. Frontiers in Sustainable Food Systems. 8, 1395730. DOI: https://doi.org/10.3389/fsufs.2024.1395730

[16] Vesely, D., 1984. Electron Beam Damage of Amorphous Synthetic Polymers. Ultramicroscopy. 14(3), 279–290. DOI: https://doi.org/10.1016/0304-3991(84)90096-2

[17] Grubb, D.T., 1974. Radiation Damage and Electron Microscopy of Organic Polymers. Journal of Materials Science. 9, 1715–1736. DOI: https://doi.org/10.1007/BF00540772

[18] Li, A., Zhang, N., Santos, R.M., 2023. Mineral Characterization Using Scanning Electron Microscopy (SEM): A Review of the Fundamentals, Advancements, and Research Directions. Applied Sciences. 13(23), 12600. DOI: https://doi.org/10.3390/app132312600

[19] Koga, D., Kusumi, S., Shibata, M., et al., 2021. Applications of Scanning Electron Microscopy Using Secondary and Backscattered Electron Signals in Neural Structure. Frontiers in Neuroanatomy. 15, 759804. DOI: https://doi.org/10.3389/fnana.2021.759804

[20] Hartmann, M.A., Blouin, S., Misof, B.M., et al., 2021. Quantitative Backscattered Electron Imaging of Bone Using a Thermionic or a Field Emission Electron Source. Calcified Tissue International. 109, 190–202. DOI: https://doi.org/10.1007/s00223-021-00832-5

[21] Butler, J.H., Joy, D.C., Bradley, G.F., et al., 1995. Low-Voltage Scanning Electron Microscopy of Polymers. Polymer. 36(9), 1781–1790. DOI: https://doi.org/10.1016/0032-3861(95)90924-Q

[22] Drummy, L.F., Yang, J., Martin, D.C., 2004. Low-Voltage Electron Microscopy of Polymer and Organic Molecular Thin Films. Ultramicroscopy. 99(4), 247–256. DOI: https://doi.org/10.1016/j.ultramic.2004.01.011

[23] Hovington, P., Drouin, D., Gauvin, R., 1997. CASINO: A New Era of Monte Carlo Code in C Language for the Electron Beam Interaction—Part I: Description of the Program. Scanning. 19(1), 1–14.

[24] Drouin, D., Hovington, P., Gauvin, R., 1997. CASINO: A New Era of Monte Carlo Code in C Language for the Electron Beam Interactions—Part II: Tabulated Values of Mott Cross Section. Scanning. 19(1), 20–28. DOI: https://doi.org/10.1002/sca.4950190103

[25] Hovington, P., Drouin, D., Gauvin, R., et al., 1997. CASINO: A New Era of Monte Carlo Code in C Language for the Electron Beam Interactions—Part III: Stopping Power at Low Energy. Scanning. 19(1), 29–35. DOI: https://doi.org/10.1002/sca.4950190104

[26] Chaudhary, N., Singh, A., Debnath, A.K., et al., 2015. Electron Beam Modified Organic Materials and Their Applications. Solid State Phenomena. 239, 72–97. DOI: https://doi.org/10.4028/www.scientific.net/SSP.239.72

[27] Singh, P.K., Venugopal, B.R., Nandini, D.R., 2018. Effect of Electron Beam Irradiation on Polymers. Journal of Modern Materials. 5(1), 24–33. DOI: https://doi.org/10.21467/jmm.5.1.24-33

[28] Shanmugharaj, A.M., Vijayabaskar, V., Bhowmick, A.K., 2022. Electron Beam Processing of Rubbers and Their Composites. International Polymer Processing. 37(5), 471–504. DOI: https://doi.org/10.1515/ipp-2021-4211

[29] Clark, D.T., Brennan, W.J., 1986. An ESCA Investigation of Low Energy Electron Beam Interactions with Polymers. I. PTFE. Journal of Electron Spectroscopy and Related Phenomena. 41(2), 399–410. DOI: https://doi.org/10.1016/0368-2048(86)85017-4

[30] Song, Z.G., Ong, C.K., Gong, H., 1997. Secondary and Backscattered Electron Yields of Polymer Surface under Electron Beam Irradiation. Applied Surface Science. 119(1–2), 169–175. DOI: https://doi.org/10.1016/S0169-4332(97)00182-7

[31] Goldstein, J.I., Newbury, D.E., Echlin, P., et al., 1992. Scanning Electron Microscopy and X-Ray Microanalysis: A Text for Biologists, Materials Scientists, and Geologists, 2nd ed. Plenum Press: New York, NY, USA. pp. 90–101.

[32] Neggers, J., Héripré, E., Bonnet, M., et al., 2021. Principal Image Decomposition for Multi-Detector Backscatter Electron Topography Reconstruction. Ultramicroscopy. 227, 113200. DOI: https://doi.org/10.1016/j.ultramic.2020.113200

[33] Jablonski, A., 1985. Elastic Backscattering of Electrons from Surfaces. Surface Science. 151(1), 166–182. DOI: https://doi.org/10.1016/0039-6028(85)90460-1

[34] Scrivener, K.L., 2004. Backscattered Electron Imaging of Cementitious Microstructures: Understanding and Quantification. Cement and Concrete Composites. 26(8), 935–945. DOI: https://doi.org/10.1016/j.cemconcomp.2004.02.029

[35] Said, N.S., Lee, W.Y., 2025. Pectin-Based Active and Smart Film Packaging: A Comprehensive Review of Recent Advancements in Antimicrobial, Antioxidant, and Smart Colorimetric Systems for Enhanced Food Preservation. Molecules. 30(5), 1144. DOI: https://doi.org/10.3390/molecules30051144

[36] Sharaby, M.R., Soliman, E.A., Abdel-Rahman, A.B., et al., 2022. Novel Pectin-Based Nanocomposite Film for Active Food Packaging Applications. Scientific Reports. 12, 20673. DOI: https://doi.org/10.1038/s41598-022-25192-4

[37] Li, P.J., Liang, J.Y., Su, D.L., et al., 2020. Green and Efficient Biosynthesis of Pectin-Based Copper Nanoparticles and Their Antimicrobial Activities. Bioprocess and Biosystems Engineering. 43, 2017–2026. DOI: https://doi.org/10.1007/s00449-020-02390-w

[38] Sreeju, N., Rufus, A., Philip, D., 2016. Microwave-Assisted Rapid Synthesis of Copper Nanoparticles with Exceptional Stability and Their Multifaceted Applications. Journal of Molecular Liquids. 221, 1008–1021. DOI: https://doi.org/10.1016/j.molliq.2016.06.080